City Research Online

City, University of London Institutional Repository

This is the accepted version of the paper.

This version of the publication may differ from the final published version.

Computational Modeling of Twin Screw Pumps for Thermal Management Applications

Gautham Ramchandran[1*], Sham Rane[2], Ahmed Kovacevic[2], Carlo Höhn[3], Sebastian Sieder[3]

[1]Gamma Technologies, LLC.
601 Oakmont Lane, Suite 220
Westmont, IL 60559 USA
+1-630-325-5848
g.ramchandran@gtisoft.com

[2]Center for Compressor Technology
City University of London, UK
+44 20 7040 8780

[3]NIDEC GPM GmbH
Schwarzbacher Straße 28
98673 Auengrund OT Merbelsrod
Germany
+49 36878 64 4283

*Corresponding Author

ABSTRACT

Electrification has become less of a catchphrase and increasingly commonplace when discussing today's locomotives. Engineers developing thermal management strategies (both component suppliers and system-level analysts) must be armed with effective tools to design and analyze essential components such as coolant pumps and study their behavior in an actual system. This study focuses on the analysis of twin screw pumps for cooling battery packs in hybrid and battery electric vehicles via three different approaches – experimental measurements, a one-dimensional (1D) thermodynamic chamber model, and a three-dimensional (3D) computational fluid dynamics (CFD) model. Experimental measurements are conducted to quantify the coolant's volume flow rate and the shaft power consumption over a range of operating speeds and pump discharge pressures. While these measurements provide some insight into the overall internal leakages and pumping efficiencies, more comprehensive tests at a higher cost are required to fully understand the detailed thermodynamic processes occurring within the pump. Two computational modeling approaches are presented and extensively validated against these measurements. The 1D chamber model demonstrates a good agreement of all measured quantities at a very low computational cost. It also provides useful information regarding the relative importance of the various leakage paths along with the working processes and pressure pulsations. This makes it an effective tool to quickly analyze operating conditions where test data may not be available and iterate towards improved designs via parametric analysis. 3D CFD yields very good agreement compared to the measured results and provides a more complete picture with greater spatial accuracy that is sacrificed in the 1D approach. However, this is available at a significantly higher computational cost. A combination of both methodologies can guide engineers in designing screw pumps for optimal performance.

1   Introduction

The automotive engineering world is undergoing a transition towards electrifying vehicles. A key objective for engineers as they design battery and hybrid electric vehicles is to keep the size of the battery as small as possible. The larger the battery, the greater are the emissions generated in producing it. Also, if the power consumed by the system is kept to a minimum, most of the battery power could be utilized towards extending driving range. In striving towards this goal, it becomes imperative to analyze the various sources of power consumption in the

system and optimize designs at a component level. In the thermal management system, the largest power consumer is the coolant pump. Therefore, it is essential for engineers – both pump suppliers and automotive system analysts – to be armed with the appropriate tools to analyze the performance of coolant pumps and optimize their designs to ensure high efficiencies. With the availability of accurate, well-validated coolant pump models, performance maps can be generated for hard-to-measure operating conditions which may then be used in cooling system models. Moreover, pump models can also aid in the accurate prediction of transient conditions including during coolant pump start-up and shut-down conditions.

To that end, this paper focuses on the analysis of twin screw coolant pumps designed for cooling battery packs in hybrid and electric vehicles. Two different approaches (a 1D thermodynamic chamber model and a 3D CFD model) are developed, validated against measured performance indicators, and compared against each other to provide engineers guidance on the state of the art approaches available today in the design and analysis of these components.

Two variants of the screw rotor pair have been evaluated in this study. The first is a metal rotor variant that has been manufactured with a design leakage gap size of 0.05 mm and the second variant is a plastic rotor with identical profiles and size, except that the design leakage size is larger at 0.1 mm in the interlobe and radial gaps. Experimental measurements available for the flow rates and pressures at different operating speeds for the two pumps have been used to validate both models. The test rig, pump, and rotors used by NIDEC GPM GmbH to obtain these measurements are shown in Figure 1.
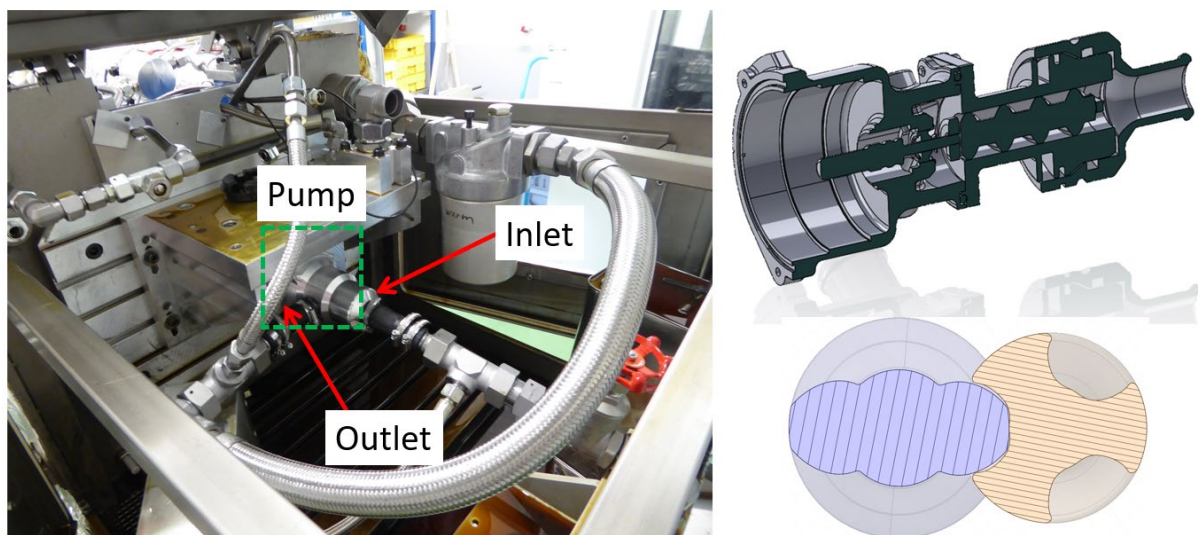
Figure 1 Test setup, pump, and rotor cross-section of the 2-3 screw pump

2   1D Thermodynamic Chamber Model
In this study, a well validated positive displacement pump modeling approach using GT-SUITE has been used for the 1D thermodynamic performance analysis. Many types of positive displacement machines have been modeled and validated with this solver in literature including gerotor pumps [1, 2], vane pumps [3], swashplate compressors [4], scroll compressors [5], etc. to name a few. In the realm of twin screw machines, single and multi-phase screw expanders have been modeled and validated with GT-SUITE [6, 7]. However, to the authors' knowledge,

this is the first study modeling the thermodynamics in a twin screw pump with the GT-SUITE solver. One advantage of the approach proposed in this study compared to other 1D models available in literature is the tight integration between the geometry calculation pre-processing tool (SCORG) and the 1D pump chamber modeling tool (GT-SUITE) and the automated workflow. This approach also allows the analyst to take advantage of the multi-physics system modeling environment available in GT-SUITE to develop the automotive cooling system and optionally integrate this with various other systems within the same tool.

2.1   Model Setup and Description

The model workflow involves the following steps:

(a) Import rotor profiles into SCORG and define all geometrical characteristics including leakage gaps, port definitions, and operating conditions.

(b) Generate volume, port area and leakage area profiles using SCORG.

(c) Run a pre-defined GT-SUITE chamber model with the generated profiles and other inputs.
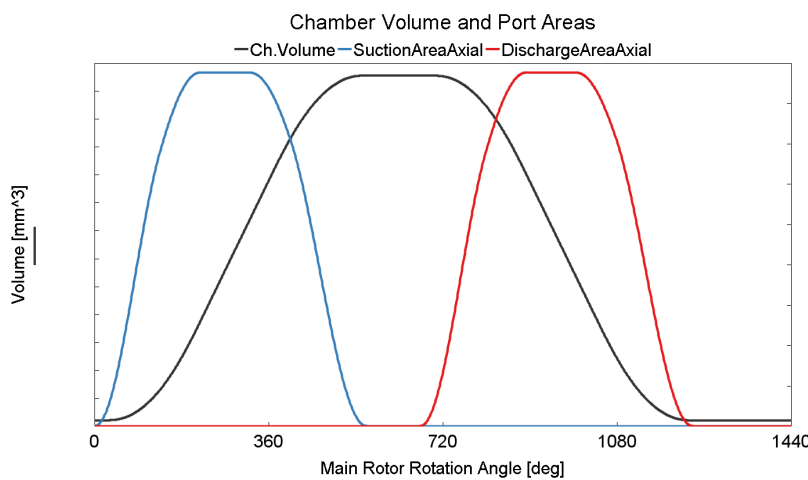

Figure 2 Chamber volume and suction and discharge port areas as functions of main rotor rotation angle
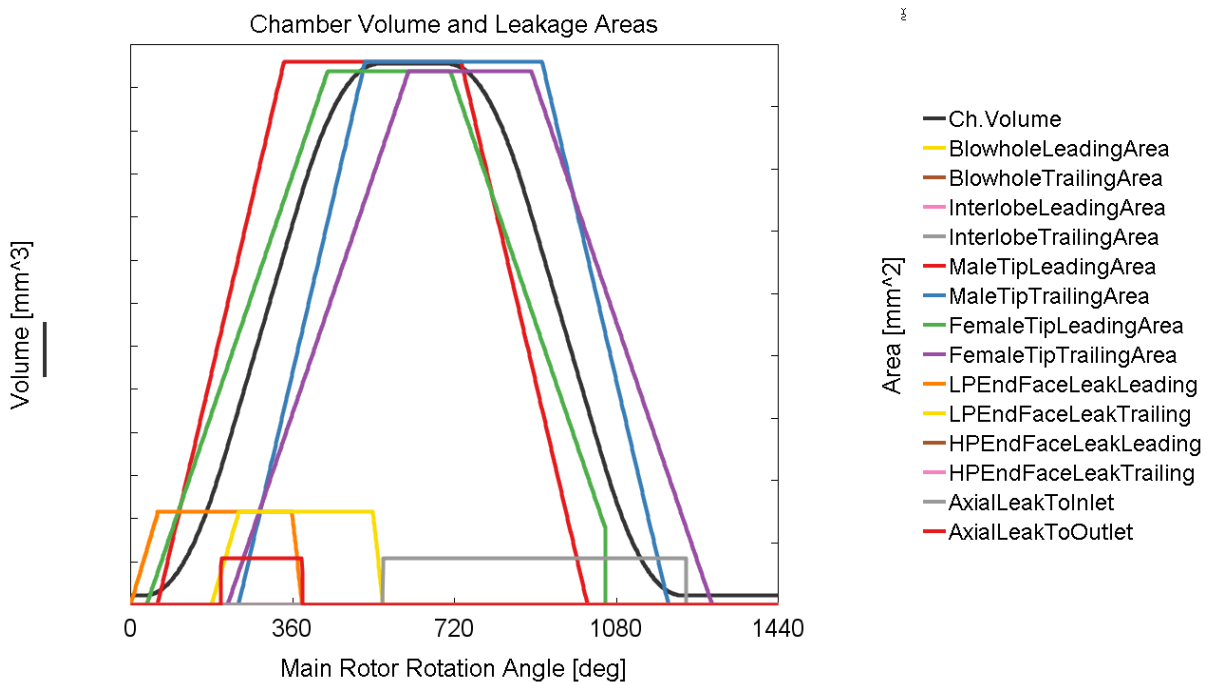

Figure 3 Chamber volume and leakage areas as functions of main rotor rotation angle

SCORG V5.9 was used in the first step of the model building process. The 2D rotor profiles are automatically extracted from the imported CAD. Geometrical inputs such as leakage gaps (radial, axial and interlobe leakages), inlet and outlet pipes and ports (radial/axial/both), boundary conditions, and working fluid are defined. Geometry calculations are then run in SCORG to generate two text files – one with the various parameters such as boundary pressures, temperatures, pump speed, pipe, and port geometry inputs, etc., and the other with the volume, port areas and leakage areas vs male rotor rotation angle, both of which the GT-SUITE model looks up automatically. Figure 2 shows the variation of the chamber volume and port areas with the male rotor rotation angle. There are only axial suction and discharge ports present in this design (no radial ports). Figure 3 shows the various leakage areas. Details of the geometrical calculations performed by SCORG to generate these profiles may be found in [8].

Optionally, a third text file may be generated containing the axial and radial bearing load profiles by running force calculations in SCORG. These profiles may be used to predict the mechanical friction losses in bearings using the advanced journal and roller bearing models available in GT-SUITE. However, the emphasis here was on the flow performance and the mechanical losses may form the subject of a future study.

Once the inputs for the chamber model are ready, the pre-built GT-SUITE model shown in Figure 4 is run either from within SCORG via a command line call or from within the GT-ISE main model building interface. GT-SUITE models are available with a varying number of working chambers. The correct model is chosen automatically by calculating the product of the number of lobes in the main rotor and the integral number of shaft rotations in one working cycle. In this study, a 2-3 lobed screw pump with four shaft rotations per working cycle results in an 8-chamber model being selected.
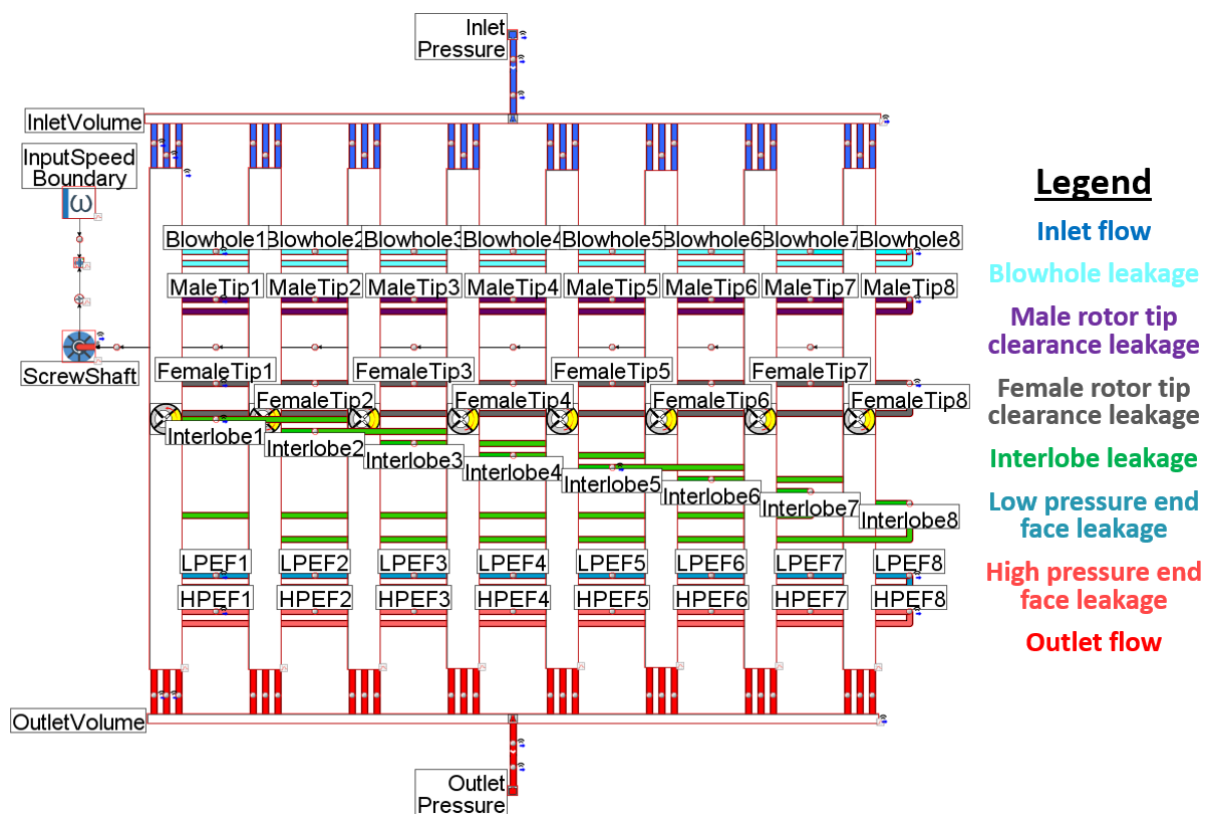

Figure 4 Schematic of the GT-SUITE model map with the chamber volumes and flow paths

The model schematic in Figure 4 highlights the flow path including the various templates used to model the screw pump. The dark blue path shows the flow from the inlet volumes entering the working chambers while the red flow path denotes the pressurized flow sent through the outlet of the pump. While the template model contains pipes and flowsplits representing generic inlet and outlet piping and volumes, these can be modified by discretizing the real flow path from 3D CAD in a semi-automatic fashion using the GEM3D pre-processor in GT-SUITE. The model also contains the various leakage paths created through the different clearances created in the screw pump. The 1D chamber models are discretized into 22 flow volumes with an average timestep size of around 1.28e-6 seconds. It takes between 30 seconds to 1.5 minutes of run time and 4 cycles for each operating condition to meet the steady state criteria imposed on mass flow rate, pressure, and temperature on a modern computer.

3   3D CFD Model

The twin screw pump has a pair of helical rotors that form a closed pumping volume between their lobes and the housing. The rotors are accurately machined such that a conjugate profile engagement occurs over the full length. Within this mechanism, leakage gaps are present between the two rotors called interlobe leakage, between the rotor tips and the housing called radial leakage and due to the helical lobes, blow-hole leakage is formed at the top and bottom housing cusps where the main and gate rotor bore diameters intersect [9]. For an accurate representation of the twin screw pump geometry, the rotor profile, helical rotor geometry and all these leakage gaps are required to be accurately generated in the computational mesh [10, 11]. A special purpose meshing tool SCORG developed at City, University of London [10, 11] has been used for this purpose. More essentially, the SCORG mesher provides pre-generated rotors grids which are then used by the CFD solver during run time for mesh deformation calculations. Details of the procedures and pre-processing requirements for such a twin screw machine using a single domain deforming grid for both the rotors and CFD analysis is reported in [11, 12] and further applications can be found in [13-17]. *Yan et al.* [15, 16, 17] have reported extensive analysis of 2-3 lobed screw pumps: from the rotor profile generation to pump design and 3D CFD analysis using SCORG grid generator and the STAR-CCM+ flow solver. In [17], they have also added a cavitation model to the screw pump analysis and have discussed the effect of high-speed operation on pump performance and prediction of cavitation zones. Similarly, fluids with widely varying viscosity and density properties were evaluated along with varying leakage gaps sizes in order to determine their sensitivity to the pump performance.

3.1   Model Description

In the current study, a well validated flow solver ANSYS CFX has been used for the performance calculation of the 2-3 lobed screw pump [11, 12]. The miniature size of the rotors of the order of 20 mm diameter, is a special characteristic of this pump and presently there is no literature available that presents an extensive analysis of such small size twin screw pumps. Due to the small rotor size, the impact of leakage flow is stronger on the volumetric efficiency of the pump. The CFD model is generated using two sets of rotor grids from SCORG with their respective design leakage gap sizes.

Figure 5 presents the main elements of the 3D transient CFD model of the screw pump. In Figure 5a, the domains and boundaries have been highlighted. The flow geometry is divided into three domains; suction port that has the inlet boundary, rotor domain is a time varying computational mesh generated using SCORG and houses the main rotor, the gate rotor and all the leakages and the third domain is the discharge port that has the outlet boundary. The three

domains are connected through non-conformal interfaces in the ANSYS CFX solver. Both inlet and outlet boundary conditions are specified pressure based on the pump's operating conditions as reported in Table 1. In Figure 5b, the computational grid of the helical main and gate rotors is presented and as shown in Figure 4c, the rotor grid deforms with time. Three rotor positions and the cross-section grids are shown in Figure 5c – c1, c2 and c3 at 0°, 45° and 90° rotations, respectively. After a cyclic rotation, the meshes are reused in the solver to simulate continuous pumping process. A grid size of 1359442 nodes has been used for the calculations.
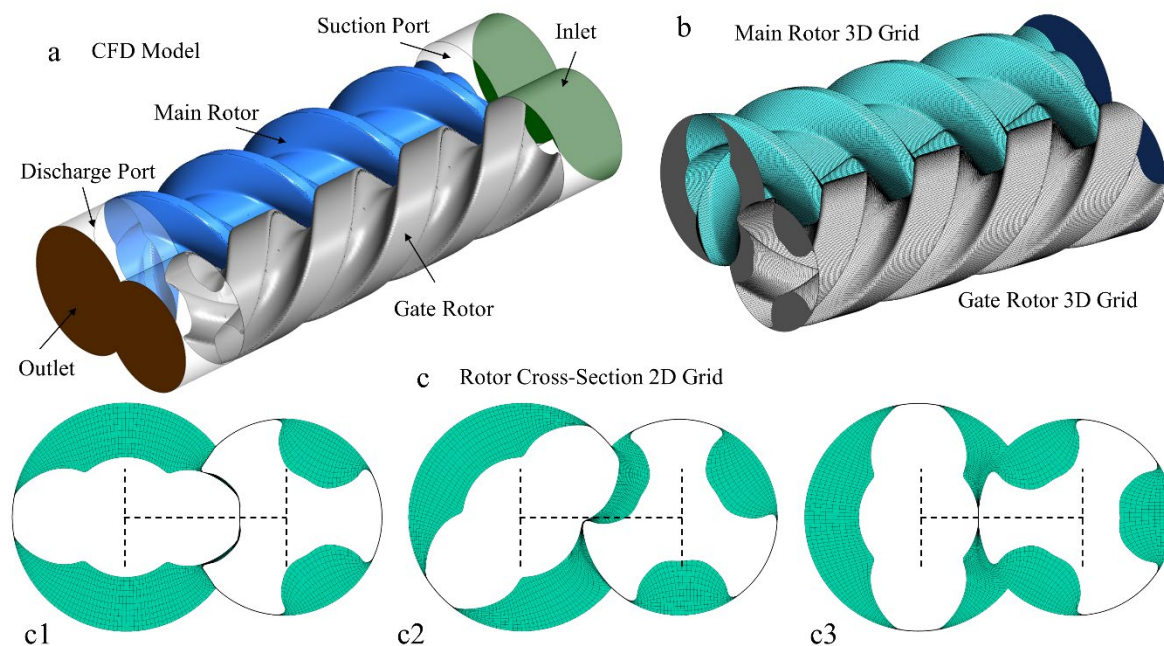
Figure 5 Computational model of the twin screw pump, a) CFD model, b) 3D rotor grid, c) 2D rotor cross-section grid at three rotor angular positions c1, c2 and c3.

GLYSANTIN engine coolant by BASF-SE, Germany, was set as the test fluid with 50% concentration of ethylene glycol and water and an operating temperature of 65°C. Accordingly, the fluid properties were set as, density of 1044 kg/m^3, specific heat capacity at constant pressure of 3550 J/kg K, a dynamic viscosity of 0.001411 kg/m s and a thermal conductivity of 0.42 W/m K. All fluid properties were set as constant in the CFD calculations.

Table 1 Specification of the numerical setup in the ANSYS CFX solver.

Mesh deformation	User defined nodal displacement	Advection scheme	High Resolution
Mesh in ports	Tetrahedral with boundary layer refinements (ANSYS Mesh)	Transient scheme	Second order Backward Euler
Turbulence model	SST – k Omega (Standard Wall Functions)	Transient inner loop coefficients	Up to 10 iterations per time step
Inlet boundary condition	Opening (Specified total pressure and temperature)	Convergence criteria	r.m.s residual level 1e^{-03}
Outlet boundary condition	Opening (Static pressure, backflow acts as total pressure and temperature)	Relaxation parameters	Solver relaxation fluids (0.4)

ANSYS CFX provides a coupling feature called Junction Box Routine that is a user defined library to specify mesh deformation from custom applications such as SCORG. The solver updates the nodes coordinates from set of pre-generated coordinate files after every crank angle step (or its submultiples). Solver time step size finally results from the selected crank angle step (at which the customized grids are generated) and revolution speed of the rotor. In the present study, a 2 degree per time step rotation was used in the mesh deformation setup. It takes about 160 minutes to complete one pumping cycle and the models were run for 4 cycles to obtain the final steady state results, taking about 10 hours to run each operating condition. The computer used for this study is a 20 core, 32 GM RAM, Intel(R) Xeon(R) CPU E5-2630 v3 @ 2.40 GHz, with 2 processors.

4   Results and Discussion

The pump performance is dependent on the leakage flow and rotor torque prediction under the varying operating conditions. Based on this, the metal screw and the plastic screw models were evaluated over a range of operating speed and pressures and the results such as internal pressure distribution and flow characteristics have been discussed here. The pump's full range performance with metal and plastic screw pairs and verification with experimental data has also been presented.

4.1   Pressure Distribution
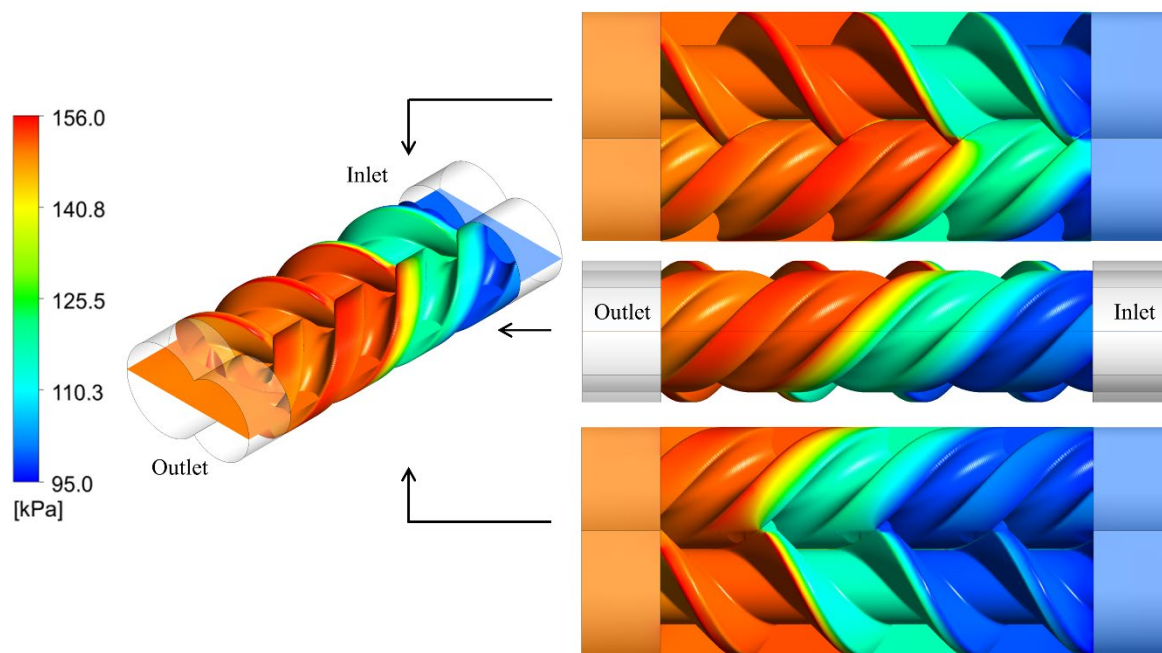
Figure 6 Pressure distribution at 3000 rpm, 1.5 bar discharge pressure with metal screw pair.

As the screw rotors rotate, successive interlobe chambers are transported from the suction end to the discharge end. There is no change in the internal volume of the trapped chamber due to this rotation but since the discharge port is at a higher pressure, the fluid pressure inside the chamber rises as soon as it opens to the discharge. In Figure 6, the nature of pressure distribution in the pump is presented at the operating speed of 3000 rpm when delivery pressure is 1.5 bar. The main rotor has a wrap angle of 675° over its length and due to its two lobes, two working chambers are simultaneously formed as shown in Figure 6. The top chamber pressure distribution lags the bottom chamber pressure by 180° phase angle. This nature of pressure

distribution results into a variable bending moment that acts on the rotors and can result into performance deviation from the ideal conditions.

Figure 6 shows that though the discharge boundary is specified at 1.5 bar pressure, due to the positive displacement nature of the pump, the local internal pressure rises to 1.56 bar. Similarly, at the suction port, the pressure has been specified as 1.0 bar. But due to the rotors forming an increasing control volume, there is a drop in local pressure to 0.95 bar. These locally higher and lower port and chamber pressures result into a higher rotor torque and thereby lower the hydraulic efficiency of the pump at a given operating condition.

A set of pressure monitoring points were located on the main rotor side along the length of the rotor and these pressure data has been plotted against the rotation angle of the main rotor at various operating conditions in Figure 7 for the metal rotor pair. Due to the 675° wrap angle on the main rotor, it can be seen that the pressure in the pump rises from suction pressure to delivery pressure in two stages. From 0° to about 250° is at suction pressure, 250° to 400° rotation is an intermediate pressure and from 400° rotation onwards is the delivery pressure.
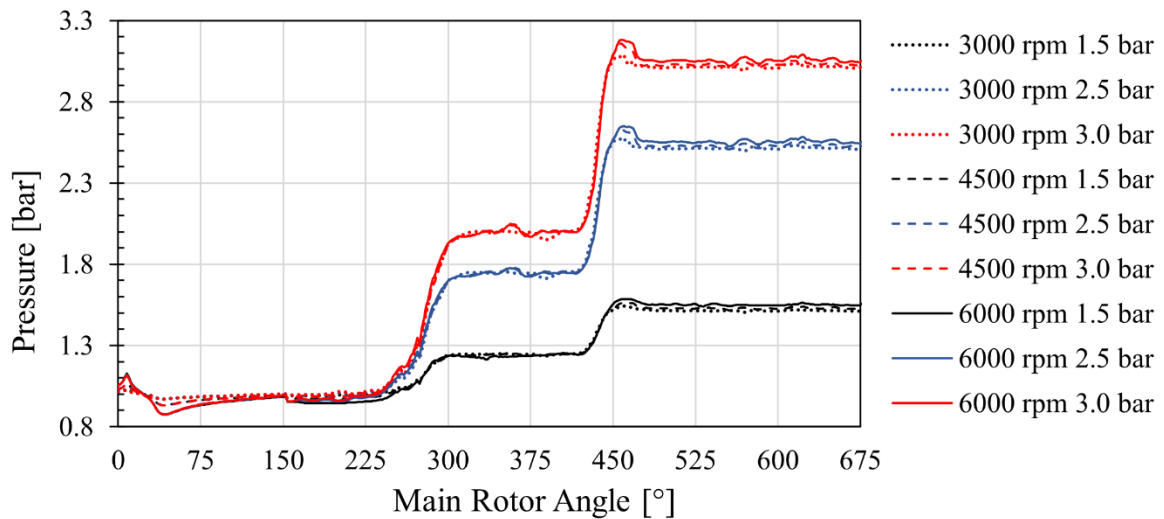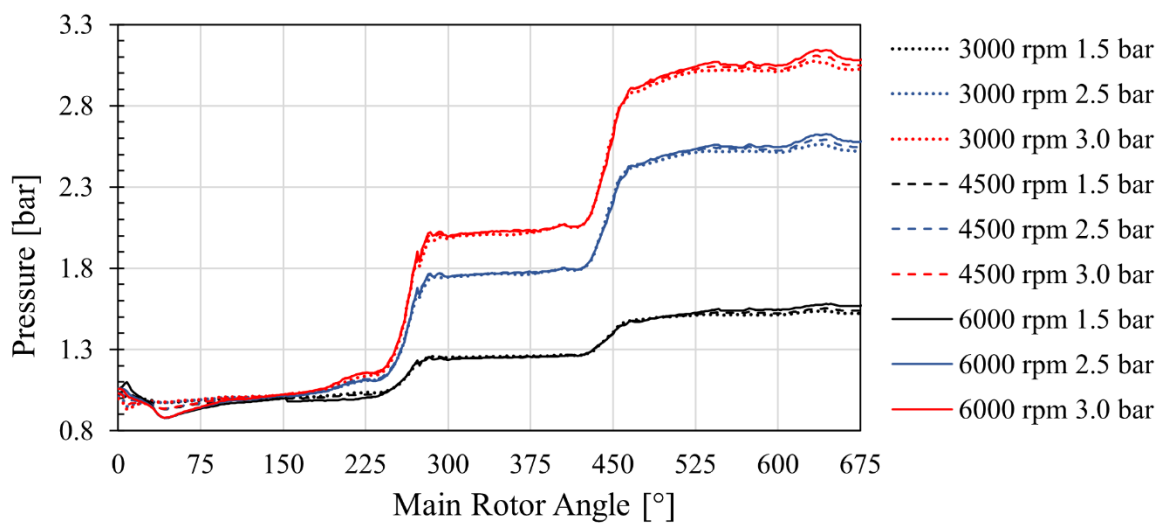

Figure 7 Pressure distribution with main rotor rotation for the metal screw pair using CFD.

It is seen from Figure 7 that the rise in pressure occurs within a 50° rotor rotation. Close to the suction, a dip in local pressure is observed at about 50° rotor angle. This dip is stronger at higher speed of 6000 rpm as compared to 3000 rpm, but not affected by the discharge pressure. While closer to the discharge at about 450° rotation, an overshoot in local pressure is seen. The overshoot is stronger at higher speed as compared to lower speed, also the overshoot is influenced by the discharge pressure, being higher at 3.0 bar as compared to 1.5 bar discharge pressure. This overshoot at 3000 rpm and 1.5 bar can be located at the leading-edge tip of the rotors in Figure 6, in their central lobe region.

Similarly, Figure 8 presents the pressure distribution data for the plastic screw pair at the same operating conditions as the metal screw. Due to the larger leakage gap size of 0.1 mm, the nature of pressure distribution is slightly altered in the plastic screws. The main characteristic of pressure rise in two stages is visible. But a noticeable difference is in the angle span of 150° to 225° rotor angle. Here the chamber pressure has already started increasing, with a larger increase seen at higher discharge pressure. This is due to the higher leakage in these rotors. The pressure rises to intermediate pressure and then to the discharge pressure more gradually in the plastic rotors as compared to the metal rotors. There is no pressure overshoot seen in the plastic rotors at all the speeds and discharge pressures. Due to this nature of pressure distribution, the rotor torque in plastic rotors is likely to be relatively lower as compared to the metal rotors. This is seen in the comparison of the performance data presented in Table 2 and Table 3.

At selected operating conditions, a one-to-one comparison of pressure distributions between the metal and plastic rotor pairs with CFD and GT-SUITE is presented in Figure 9 and Figure 10. In the case of the plastic rotors, the first pressure rise starts at an earlier rotor angle, and this tends to transition earlier at higher discharge pressures. The second pressure rise starts in both rotors at nearly the same angle close to 400° rotor position. However, with metal rotors, a steeper pressure rise is clearly seen across all the speeds and discharge pressures. These aspects of the pump's working process are identical in both numerical approaches.
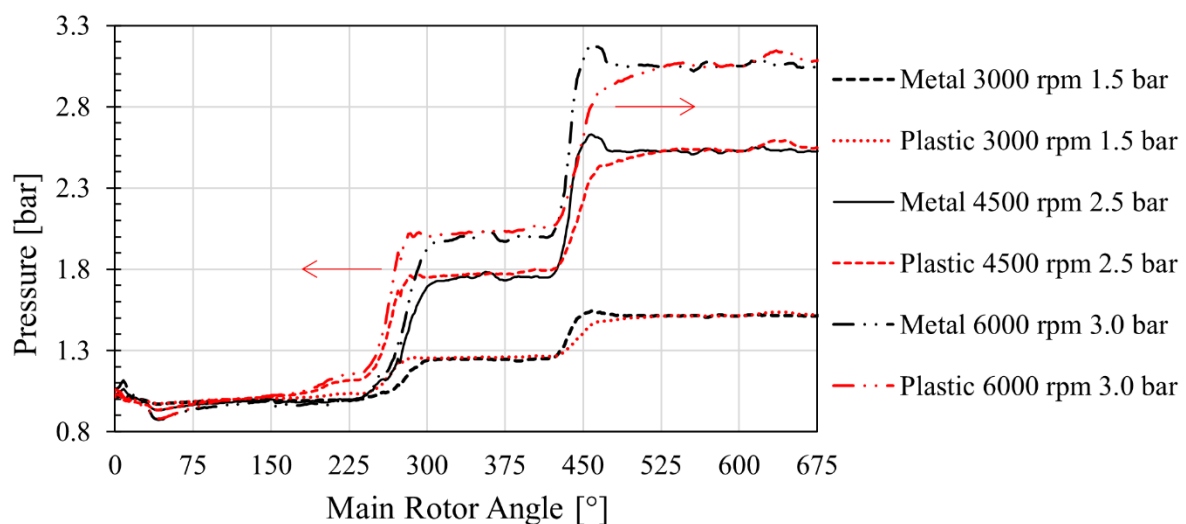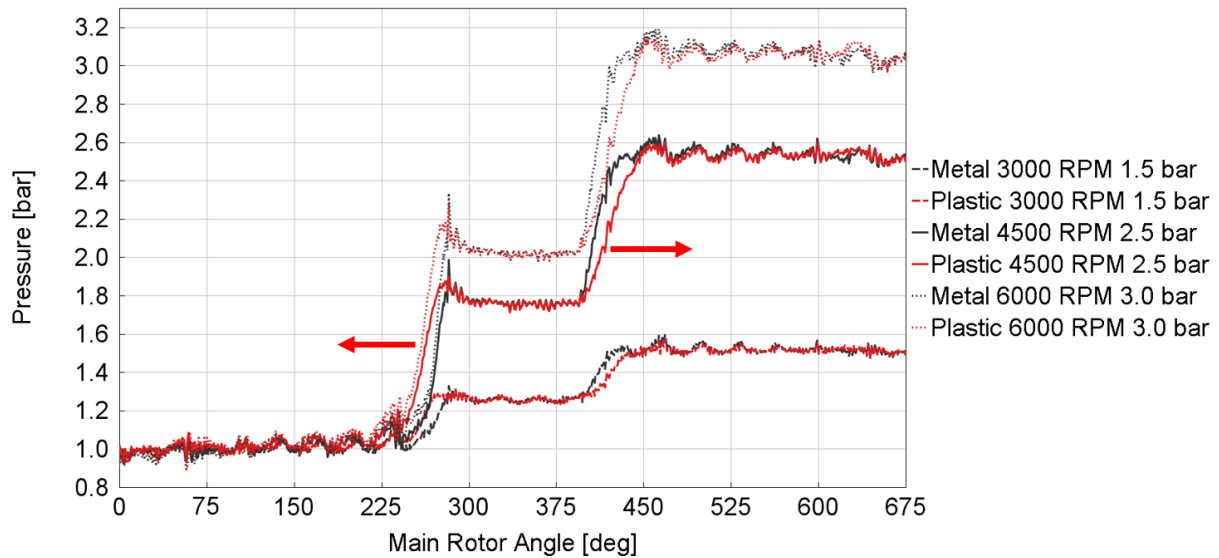
Figure 10 Comparison of pressure distribution between the metal and plastic screw pairs using GT-SUITE.

Although overall trends are similar in both the GT-SUITE and CFD comparisons, there are a few minor differences observed. CFD predicts a clear initial dip in pressure in the suction port which is present in both the rotors. While the pressure does drop below 1.0 bar at the suction port in the GT-SUITE results, it tends to fluctuate. There is a slight pressure overshoot seen in the metal rotors with CFD close to 450°. In the case of the GT-SUITE model, this is not observed.

4.2   Pump Flow Characteristics

Two pumping chambers are continuously operating in the 2-3 screw rotor pump. This results into a pulsating flow. The flow characteristic can be closely studied by monitoring the flow velocity and direction at the rotor ends with the CFD model. In Figure 11, the velocity distribution is presented in a longitudinal plane passing through the main rotor axis. The region at the outlet port is shown at incremental rotor angles from 0° to 180° which represents a pumping cycle. The region at the suction port is presented at 180° that also corresponds to 0° rotor angle. The results are at an operating condition of 3000 rpm and 1.5 bar discharge pressure.
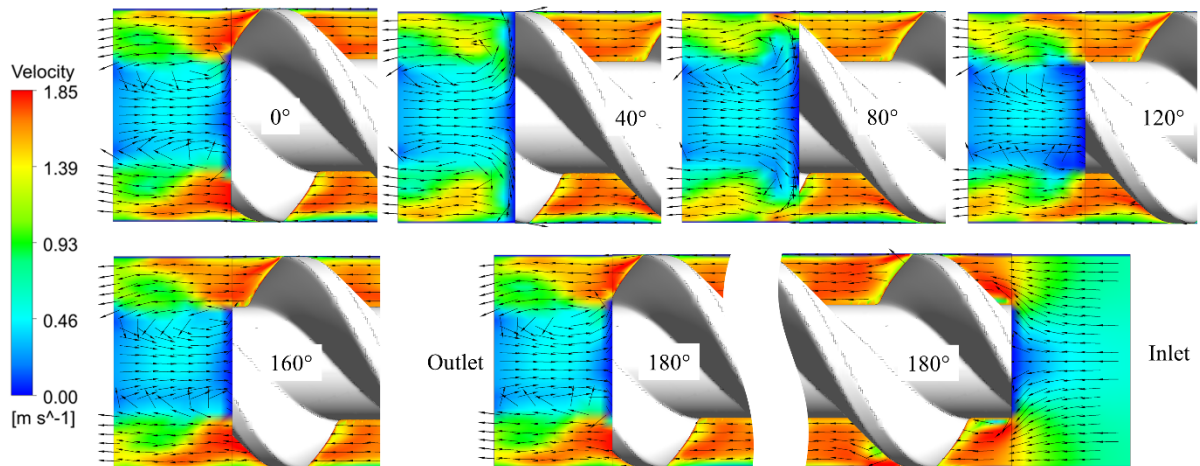
At initial rotor position of 0°, two chambers at the top and bottom of the rotor are still trapped between the rotor and the housing. The fluid velocity in the rotors is close to 1.85 m/s and in the port the velocity vectors are directed outwards. With further rotation to 40°, these chambers are just about to connect with the discharge ports. A recirculation region is getting formed and there is lower flow velocity in the port. At 80°, the chambers are connected to the port. At 120°, the flow from the chambers is delivered to the ports and flow velocity is seen to increase to 1.8 m/s. From 160° to 180°, the complete chamber volume is transported to the discharge port. This pulsating flow with recirculation zone is cyclically repeating in the discharge port. However, the flow in the suction port is uniform and the peak velocity is also lower of the order of 0.9 m/s. Within the rotors, the flow direction is uniform, and the peak velocity is of the order 1.85 m/s. Similar flow features can be observed at other operating conditions of the pump.
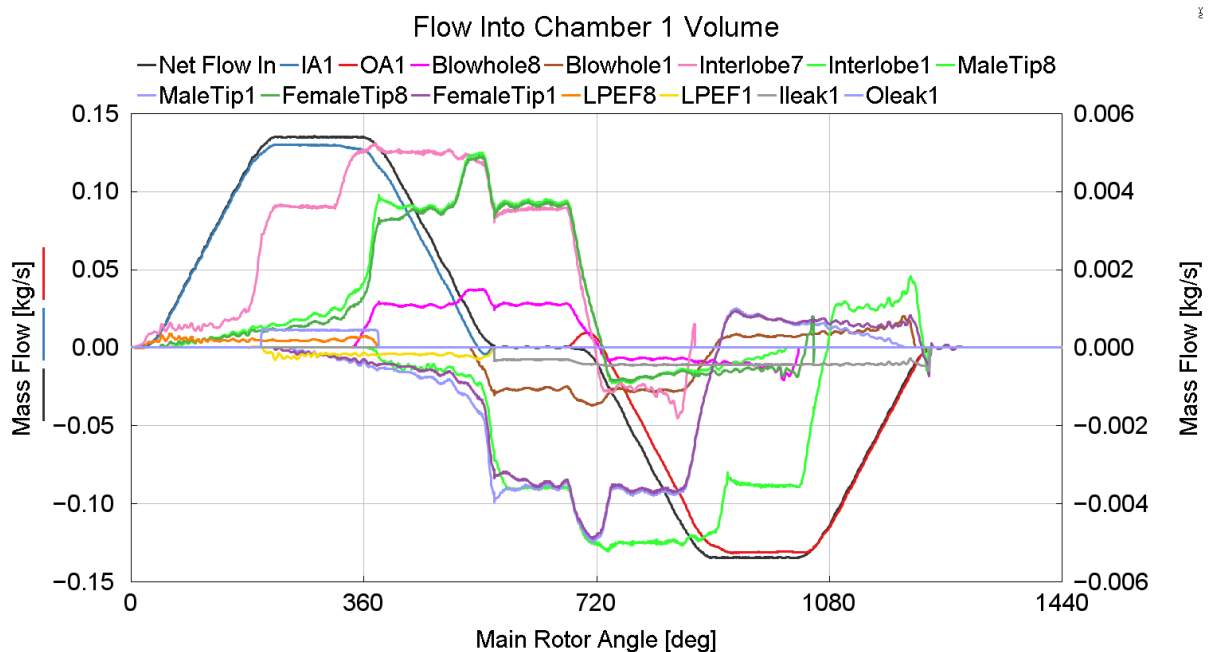
Figure 12 Mass flow into and out of the chamber volume at 3000 rpm and 1.5 bar discharge pressure.

While the GT-SUITE 1D chamber model does not provide the level of detail available from CFD, there are some useful insights that can nevertheless be gleaned. For instance, the mass flow rate entering or leaving each chamber volume via the various flow paths can be better understood. This is illustrated in Figure 12 and can provide insights into which leakage paths dominate, when each path opens and closes to the chamber, and where gains can be made while optimizing the design.

4.3   Pump Performance
The integral performance parameters of the twin screw pump are flow, power, volumetric efficiency, and hydraulic efficiency. These performance data were evaluated at various operating speeds and discharge pressures with both the CFD and GT-SUITE models.

The measured data of flow at corresponding conditions was available for the metal rotors and has been used to compare against the CFD data in Table 2 and against the GT-SUITE data in Table 3. Over the entire operating range, the flow deviation is within 6% for both CFD and GT-SUITE models. It is highest at the low speed, high pressure operating condition of 3000

rpm and 3.0 bar since the impact of leakage is the highest at these conditions. It is also observed that the hydraulic efficiencies predicted by the GT-SUITE model are greater at higher speeds. This is because the pressure overshoot observed in the CFD model is not seen in the GT-SUITE model thereby resulting in lower fluid power values and higher hydraulic efficiencies in comparison.

Table 2 CFD model performance data for metal screw pair at test conditions.

No	Speed	Discharge Pressure	Flow	Power	Volumetric Efficiency	Flow Deviation	Hydraulic Efficiency
	rpm	bar	lpm	W	%	%	%
1		1.5	13.67	14.40	91.68	3.16	79.14
2	3000	2.5	12.95	38.69	86.83	4.07	83.68
3		3.0	12.68	50.84	85.04	4.92	83.17
4		1.5	20.95	24.88	93.64	2.65	70.18
5	4500	2.5	20.23	61.32	90.44	3.00	82.49
6		3.0	19.96	79.56	89.24	3.23	83.65
7		1.5	28.20	38.80	94.55	2.51	60.58
8	6000	2.5	27.52	87.36	92.27	2.61	78.76
9		3.0	27.26	111.66	91.37	2.72	81.36

Table 3 GT-SUITE model performance data for metal screw pair at test conditions.

No	Speed	Discharge Pressure	Flow	Power	Volumetric Efficiency	Flow Deviation	Hydraulic Efficiency
	rpm	bar	lpm	W	%	%	%
1		1.5	13.69	13.85	91.32	3.04	82.37
2	3000	2.5	12.88	38.51	85.92	4.59	83.61
3		3.0	12.58	50.83	83.94	5.67	82.50
4		1.5	21.09	19.11	94.12	2.02	91.97
5	4500	2.5	20.28	56.02	90.52	2.78	90.50
6		3.0	19.98	76.56	89.20	3.13	87.00
7		1.5	28.54	26.66	95.73	1.34	89.21
8	6000	2.5	27.69	75.42	92.85	2.03	91.79
9		3.0	27.38	99.93	91.84	2.28	91.33

In the case of the plastic rotor pair, the measured flow data was available at two operating speeds of 4000 rpm and 5900 rpm and at 2.7 bar discharge pressure. Hence, the CFD and GT models were compared at these conditions as presented in Table 4 and Table 5, respectively. The flow estimated by both models are within 2% deviation from the measured data. Additionally, the plastic rotor was evaluated at the same operating conditions as the metal rotor pair to compare the performance deviation under similar conditions. A consistently higher flow due to lower leakage gap of 0.05 mm can be observed in the metal rotors as compared to the plastic rotors with 0.1 mm leakage gap. This results in a significantly lower volumetric efficiency in the plastic rotors. Since there is no pressure overshoot observed with the plastic

rotors in both CFD and GT-SUITE (Figures 9 and 10), the power and hydraulic efficiency predictions are comparable across all operating conditions as seen from Tables 4 and 5. As discussed in the results of pressure distribution, an overshoot and steeper pressure rise in the metal rotors has resulted in higher pump power at all operating conditions as compared to the plastic rotors. However, due to the much larger flow through the metal rotors, the hydraulic efficiency of the metal rotors is higher than the plastic rotors. The difference is significant at higher discharge pressures.

Table 4 CFD model performance data for plastic screw pair.

No	Speed	Discharge Pressure	Flow	Power	Volumetric Efficiency	Flow Deviation	Hydraulic Efficiency
	rpm	bar	lpm	W	%	%	%
At test conditions:							
1	4000	2.7	12.98	57.98	65.25	1.17	63.41
2	5900	2.7	22.34	89.10	76.15	1.77	71.04
At metal screw test conditions (Table 2):							
1		1.5	11.40	13.30	76.40	-	71.38
2	3000	2.5	8.49	37.86	56.91	-	56.04
3		3.0	7.40	50.15	49.59	-	49.17
4		1.5	18.80	21.55	84.02	-	72.70
5	4500	2.5	15.89	58.47	71.04	-	67.96
6		3.0	14.81	76.91	66.18	-	64.17
7		1.5	26.16	31.69	87.70	-	68.80
8	6000	2.5	23.29	80.90	78.07	-	71.97
9		3.0	22.20	105.50	74.43	-	70.15

Table 5 GT-SUITE model performance data for plastic screw pair.

No	Speed	Discharge Pressure	Flow	Power	Volumetric Efficiency	Flow Deviation	Hydraulic Efficiency
	rpm	bar	lpm	W	%	%	%
At test conditions:							
1	4000	2.7	13.01	57.37	65.29	0.88	64.25
2	5900	2.7	22.34	86.16	76.20	1.74	73.46
At metal screw test conditions (Table 3):							
1		1.5	11.14	13.29	74.34	-	69.85
2	3000	2.5	8.50	37.84	56.70	-	56.16
3		3.0	7.53	50.12	50.22	-	50.08
4		1.5	18.50	20.73	82.58	-	74.37
5	4500	2.5	15.87	57.44	70.86	-	69.07
6		3.0	14.91	75.87	66.54	-	65.51
7		1.5	25.82	27.54	86.59	-	78.13
8	6000	2.5	23.25	78.04	77.96	-	74.48
9		3.0	22.28	102.58	74.71	-	72.40

5   Conclusions

This study of twin screw liquid coolant pumps utilizes numerical and experimental methodologies to fully characterize their fluid and thermodynamic performance over a wide range of operating conditions and to assess the robustness and validity of the GT-SUITE 1D chamber model and a 3D CFD model. The 3D CFD model provides detailed insights into the flow characteristics and pressures during pump operation. Both models are compared to measurements of the overall pump performance in terms of the volume flow rate over a range of operating pump speeds. Both models yield good agreement, within 6% deviation. The model results are further compared with each other to understand the minor differences and to gauge how well the actual working process in the pump is modeled.

This work demonstrates both methodologies as valid approaches for modeling twin screw coolant pumps. The 1D chamber model provides a very accurate model with low computational cost and suitable for design purposes and aid in quick optimization and pump performance map generation for use in system models. The 3D CFD model benefits through a more detailed prediction of the spatially dependent processes such as internal chamber pressure fluctuations, but at a larger computational cost. Both tools are valuable for the design, optimization, and analysis of twin screw coolant pumps amidst a need for state-of-the-art tools in the swift race towards electrification.

References

1. Harrison, J., Aihara, R., and Eisele, F. (2016). Modeling Gerotor Oil Pumps in 1D to Predict Performance with Known Operating Clearances, *SAE Int. J. Engines*, vol 9(3), p 1839-1846. doi: 10.4271/2016-01-1081.
2. Buono, D., di Cola, F. D. S., Senatore, A., Frosina, E., Buccilli, G., and Harrison, J. (2016). Modelling Approach on a Gerotor Pump Working in Cavitation Conditions, *Energy Procedia*, vol 101, p 701-709. doi: 10.1016/j.egypro.2016.11.089.
3. Harrison, J., Aihara, R., Eshraghi, M., and Dmitrieva, I. (2014). Modeling Engine Oil Variable Displacement Vane Pumps in 1D to Predict Performance, Pulsations, and Friction, SAE Technical Paper 2014-01-1086. doi: 10.4271/2014-01-1086.
4. Ramchandran, G., Bhatia, K., and Aihara, R. (2018). Simulation of 1D Flow Coupled with 3D Multi-Body Dynamics Model of a Double-Acting Swashplate Compressor, International Compressor Engineering Conference at Purdue, 2623.
5. Harrison, J. N., Koester, S., Aihara, R., and Ratner, D. (2018). From CAD to 1D: A Direct Approach to Modeling Scroll Compressors with Multi-Physics Simulation, International Compressor Engineering Conference at Purdue, 2539.
6. Bianchi, G., Marchionni, M., Kennedy, S., Miller, J., and Tassou, S. (2019). One-Dimensional Modelling of a Trilateral Flash Cycle System with Two-Phase Twin-Screw Expanders for Industrial Low-Grade Heat to Power Conversion, *Designs*, vol 3: 41. doi: 10.3390/designs3030041.
7. Vimalakanthan, K., Read, M., and Kovacevic, A. (2020a). Numerical Modelling and Experimental Validation of Twin-Screw Expanders, *Energies*, vol 13(18), 4700. doi: 10.3390/en13184700.
8. Stosic, N., Smith, I. K., and Kovacevic, A. (2005). *Screw Compressors, Mathematical Modeling and Performance Calculation*, Monograph, Springer Verlag Berlin.
9. Kovačević, A., Stošić, N. and Smith, I. K. (2007). *Screw compressors - Three dimensional computational fluid dynamics and solid fluid interaction*, ISBN 3-540-36302-5, Springer-Verlag Berlin Heidelberg New York.

10. Kovačević, A. (2005). Boundary Adaptation in Grid Generation for CFD Analysis of Screw Compressors, *Int. Num. Eng.*, 64(3), 401-426.

11. Rane, S. and Kovačević, A. (2017). Algebraic generation of single domain computational grid for twin screw machines. Part I. Implementation, *Advances in Engineering Software*, vol 107, p 38-50. doi: 10.1016/j.advengsoft.2017.02.003

12. Kovačević, A. and Rane, S. (2017). Algebraic generation of single domain computational grid for twin screw machines Part II – Validation, *Advances in Engineering Software*, vol 109, p 31–43. doi: 10.1016/j.advengsoft.2017.03.001

13. Rane, S. and Kovačević, A. (2017). Application of numerical grid generation for improved CFD analysis of multiphase screw machines, 10th International conference on compressors and their systems, London, IOP Conf. Ser.: *Mater. Sci. Eng.*, 232, 01. doi: 10.1088/1757-899X/232/1/012017

14. Rane, S., Kovačević, A., Stošić, N. and Smith, I. (2021). Analysis of real gas equation of state for CFD modelling of twin screw expanders with R245fa, R290, R1336mzz(Z) and R1233zd(E). *International Journal of Refrigeration*. vol 121, p 313-326. doi: 10.1016/j.ijrefrig.2020.10.022.

15. Yan, D., Kovačević, A., Tang, Q., Rane, S. and Zhang, W. (2016). Numerical modelling of twin-screw pumps based on computational fluid dynamics. Proceedings of the Institution of Mechanical Engineers, Part C: Journal of Mechanical Engineering Science. vol 231 (24), p 4617-4634. doi: 10.1177/0954406216670684

16. Yan, D., Tang, Q., Kovačević, A., Rane, S. and Pei L., (2017). Rotor profile design and numerical analysis of 2–3 type multiphase twin-screw pumps. Proceedings of the Institution of Mechanical Engineers, Part E: Journal of Process Mechanical Engineering. vol 232 (2), p 186-202. doi: 10.1177/0954408917691798

17. Yan, D., Kovačević, A., Tang, Q., and Rane S., (2018). Numerical investigation of cavitation in twin-screw pumps. Proceedings of the Institution of Mechanical Engineers, Part C: Journal of Mechanical Engineering Science. vol 232 (20), p 3733-3750. doi: 10.1177/0954406217740927